

Multi-strange Baryon Correlations at RHIC

Betty I. Abelev (for the STAR Collaboration)

University of Illinois at Chicago, Chicago, IL

Abstract. Multi-strange baryon azimuthal correlations were observed in $d+Au$ and $Au+Au$ data taken by the STAR detector at RHIC. We extract the same-side per-trigger yields for a variety of strange particle species and trigger p_{\perp} , but do not observe any species dependence. We also report the observation of an elongation in the $\Delta\eta$ direction of the Ξ correlation peak, the ridge. Comparing the same-side yields in $d+Au$ and $Au+Au$ data, we conclude that the same-side yield of the azimuthal-only Ξ correlations is greatly enhanced by the ridge yield. We also report the first observation of a strong same-side peak in the Ω baryon triggered azimuthal correlations.

Keywords: Recombination, correlations, ridge, multi-strange, RHIC, STAR
PACS: 13.60, 13.87, 14.20, 14.65, 25.75.Dw, 25.75.Gz

1. Introduction

In the heavy-ion collisions produced at Relativistic Heavy Ion Collider (RHIC) in Brookhaven National Laboratory, we observe a formation of a very dense, hot medium. The formation of this medium is manifested, among other effects, by copious production of strange quarks and anti-quarks.

An enhancement of strange particle production has long been predicted as a signature of a large thermalized system with partonic degrees of freedom [1]. The argument runs two-fold. Firstly, the threshold for strangeness production in a partonic medium is the mass of a strange quark-antiquark pair (~ 200 MeV). This is less than half the energy threshold of strangeness production in a hadron gas. Secondly, due to the comparatively large volume of the central $Au+Au$ interaction region, the system can be described by a grand-canonical ensemble, which makes the production of strange particles relatively easier the more strangeness they contain. Thus, we would expect a proportionally larger number of Ω (sss) and Ξ (ssd) baryons in most central $Au+Au$ collisions than, for example, in $d+Au$. Indeed, this has been observed [2]. However, there is much to learn about particle-production mechanisms in this medium. One of the puzzles to come out of RHIC is the enhancement

of the baryon to meson ratio at intermediate p_{\perp} ($2 < p_{\perp} < 6$ GeV/ c) in the most head-on Au+Au collisions with respect to the ratio observed in $p + p$ and the most peripheral Au+Au collisions [2]. This enhancement seems to be qualitatively explained by coalescence-recombination models [2]. A typical recombination model calculates the contributions of the soft and hard parton production to a given particle spectra. One of the recombination models, proposed by Hwa et al., [3] predicts that the vast majority of Ω baryons produced in the intermediate p_{\perp} region are from recombination and not from fragmentation. The authors also suggest that we can test the extent of the soft production of the s-quark by using the azimuthal correlations with Ω triggers. Azimuthal correlations allow us to study jet production statistically, without full reconstruction of the jet energy. The back-to-back jets manifest themselves as Gaussian peaks, separated by π radians in azimuth. In the Hwa model no such peaks would be observable due to the overwhelming majority of the Ω triggers emanating from “soft” sources.

In this work we examine this assumption and present an azimuthal correlation with a non-negligible Ω triggered same-side peak. We also present Ξ baryon correlations, where the statistics are more abundant and thus a closer examination of a result is possible.

2. Data and the experimental setup

2.1. Data

The data presented in this study were obtained in the third (d +Au) and fourth (Au+Au) year of RHIC operations, using the STAR detector [4]. Both data sets were taken at $\sqrt{s_{NN}} = 200$ GeV. Whereas the 20 million d +Au events used in the analysis came from a minimum bias data sample, the 24 million Au+Au events presented were obtained using the STAR central trigger. This trigger setup uses the number of forward neutrons that remain after the collision to estimate the impact parameter and thus the collision’s centrality. The fraction of the total cross-section that corresponds to this trigger is 0-12% most central (or most violent, i.e., events with the smallest impact parameter) events. However, only the events that matched the charged track multiplicities of the minimum bias 0-10% sample were used. In the d +Au data, to avoid pile-up events, the STAR Central Trigger Barrel (CTB) was used ensuring that all particles used in a correlation came from the same event (all particles had to pass through the CTB at the same time). In the Au+Au data, the accepted event vertex was restricted to ± 25 cm from the center of the detector. For the d +Au data set, all usable events were within 50 cm of the detector center.

2.2. Tracking and particle reconstruction

The main component of the STAR detector is its large acceptance Time Projection Chamber (TPC) [5], which covers 2π radians in azimuth and 3.6 units of pseudorapidity. The TPC is situated inside a 0.5 T solenoidal magnetic field, which allows

for the determination of charged particle momenta starting from transverse momenta of 100 MeV/c and identification of kaons, pions and protons using their energy loss (dE/dx) in the TPC gas.

The identification of strange baryons is done using the geometries of their most abundant channel decay topologies, $\Xi^\pm \rightarrow \Lambda^0 + \pi^\pm$ (99.9%) and $\Omega^\pm \rightarrow \Lambda^0 + K^\pm$ (68%). First, the Λ is identified via its characteristic V-shaped decay. Then, using the dE/dx identified pions or kaons, each multi-strange baryon is reconstructed by selecting meson- Λ pairs that fit our selection criteria of a secondary cascade vertex.

3. Analysis method

3.1. Constructing a correlation

The correlation function is composed of particle pairs, made up of *trigger* and *associated* particles. In the study presented, the trigger particle is the multi-strange baryon, and the associated particle is any primary (i.e., originating at the collision vertex) charged hadron from the same event that is not a decay daughter of the trigger particle. Since the trigger hadron is assumed to be the leading particle in a jet, its p_\perp is always higher than the p_\perp of the associated particle.

The correlation is constructed as follows: using the geometry of a multi-strange baryon decay, we calculate the invariant mass of our candidates that fall in the pre-specified p_\perp range, and select only the ones that fall under the mass peak (the actual resolution depends on the particle and the data set). The candidates must originate at the collision vertex. After we select the trigger candidate, the same event is scanned for an associated track with p_\perp greater than a pre-set threshold (1.5 GeV/c in all cases, except 2-dimensional correlations), but less than the p_\perp of the trigger. Then we calculate the azimuthal angle of each at the collision vertex, and then calculate the difference ($\Delta\phi$) between the two. Similarly, we calculate the $\Delta\eta$ of the two particles. We correct each correlation by the efficiency of finding a charged track at a given p_\perp . In d +Au data the efficiency is a uniform 89% for $p_\perp > 1.5$ GeV/c. For Au+Au data the efficiency varied from 72 to 78% depending on the centrality of the event and the p_\perp of the charged track. We also correct the entire correlation function for detector acceptance in both azimuth and pseudo-rapidity. This is done by first constructing a correlation function by combining random trigger and associated particles from separate pools collected over all events. The correction function is then normalized to its maximum value and the true correlation function is then divided by this constructed correction function.

3.2. Background subtraction: Flow determination

In Au+Au collisions, the underlying background shape is a direct consequence of the azimuthal anisotropy of the collision and of the underlying partonic flow. The 2nd harmonic of the elliptic flow is sinusoidal in shape and can be described by expression 1:

$$B \times 2v_2^{assoc}v_2^{trigg} \cos 2\Delta\phi \quad (1)$$

where B is the height of the uncorrelated background, and v_2^{assoc} and v_2^{trigg} are the second harmonic coefficients of the Fourier expansion of the elliptic flow for trigger and associated particles respectfully. In STAR, there are several distinct methods for elliptic flow determination. The most commonly used are the 4-particle cumulant ($v_2\{4\}$), and the so-called ‘‘Reaction Plane’’ methods [6]. Due to the small eccentricity of the overlap region, the two methods give v_2 values that can be as much as 50% apart for the 0-5% central Au+Au data. Thus, in order to determine background fluctuation we use the average of the two values, and then use the maximum and minimum values to estimate the systematic uncertainty in the yield measurement. For the purposes of the study, we assume constituent quark scaling [7], and use the v_2 measured for pions. Thus the difference in the background between the species is due only to the difference in the level of the uncorrelated background, which will be discussed in the next section.

3.3. Background subtraction: Setting the background level

In each collision system considered here, there was a large uncorrelated background associated with each correlation function. The height of the background can either be measured by fitting the correlation function, or by assuming Zero Yield At Minimum (ZYAM) [8]. The ZYAM method works under the assumption that at the minimum x_{min} of the correlation function, $C_n(\Delta\phi)$, $C_n(x_{min})$ is due only to background. The determination of the function’s minimum and the differences between a free fit and a ZYAM calculation, introduce an additional source of systematic uncertainty on the same-side yield. In the d +Au data the statistics were scarce and thus the statistical error bars on the data points were too large to constrain x_{min} precisely. Thus only a periodic fit with an ansatz as shown in equation 2 was used.

$$C_n(\Delta\phi) = A_0e^{-\Delta\phi^2/2\sigma} + A_0e^{-(\Delta\phi-\pi)^2/2\sigma} + B \quad (2)$$

In Au+Au data the ansatz had an additional term: B in equation 2 was replaced by $B \times (1 + 2v_2^{assoc}v_2^{trigg} \cos 2\Delta\phi)$. Using this ansatz, we calculate the v_2 coefficients associated with the given mean p_\perp of the trigger and associated particles. We then estimate the minima of the correlation function by fitting two, three or four points around the trough. We then set our ansatz equation to zero and calculate B . At this point we know the underlying term completely, and can subtract the background function point by point from the experimental correlation function. We then fit the same-side of the result using a Gaussian, and calculate the yield.

4. Results

Multi-strange baryon azimuthal correlations were observed in d +Au and Au+Au data and same-side yields extracted for a variety of trigger p_\perp . Figure 1 shows the

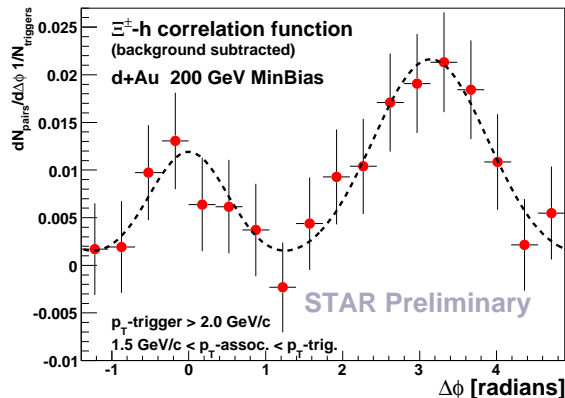


Fig. 1. Ξ^\pm -h correlation function in $\sqrt{s_{NN}}=200$ GeV $d+Au$ data, normalized by the number of triggers. The function is shown after background subtraction. The dashed curve shows the two-gaussian free fit to the data, from which the yields were extracted. All Ξ triggers are at $p_\perp > 2$ GeV/c, all associated particles have 1.5 GeV/c $< p_\perp < p_\perp$ -trigger.

correlation function constructed using Ξ baryons triggers in $d+Au$ data. To gain more statistics, the trigger p_\perp threshold was lowered to 2 GeV/c. The statistics are still scarce, but after fitting the correlation function as described in section 3.3, we were able to extract the same side-yield per trigger, which was 0.015 ± 0.026 . This is approximately ten times smaller than the same-side yield obtained at the same trigger and associated particle p_\perp in 0-10% central Au+Au data (0.20 ± 0.05).

Looking at the Au+Au Ξ correlation function in two dimensions (as shown in Figure 2), we see that the peak around $\Delta\phi=0$ is elongated in $\Delta\eta$. This underlying structure, or ridge, has been previously observed in correlations constructed using charged particles and Λ baryons. This is the first observation of this effect for multi-strange triggered correlations. To separate any jet peak from the underlying ridge, we divide the 2-dimensional phase-space into a jet+ridge and ridge-only regions. We then subtract the ridge-only space from that where both jet and ridge are present. The method has been effectively used previously for Λ and charged particles [9]. However, in the case of multi-strange baryons, the statistics are insufficient to extract the jet yield from the jet+ridge combination. From measurements of Λ and K_S^0 , [9] we know that at similar p_\perp -trigger and p_\perp -associated, the jet yield is approximately independent of the size of the collision. Assuming this holds true for the multi-strange particles, we can approximate the contribution of the ridge to the yield by comparing the $d+Au$ yields to those obtained at similar p_\perp trigger in central Au+Au. Comparing the two yields, we observe that at least 90% of the same-side Ξ correlation peak in central Au+Au comes from the ridge.

Given the prediction in [3], we would expect that the same-side peak observed in Ξ correlations is due to the non-strange quark present in the Ξ baryon. We therefore look at the triply-strange Ω baryons to test the prediction. Following the

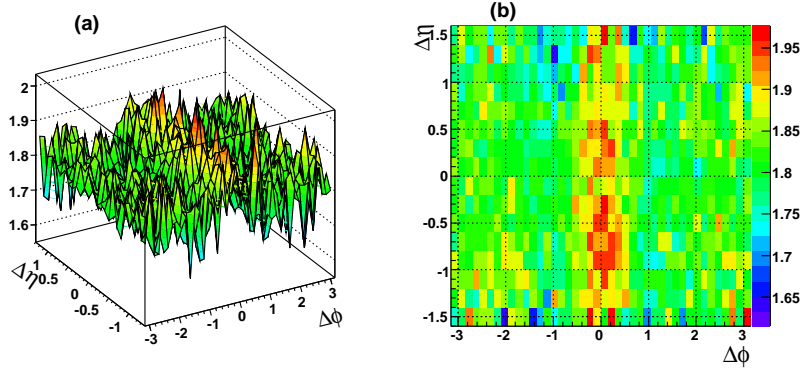


Fig. 2. $\Delta\eta$ - $\Delta\phi$ correlation with Ξ triggers with $2.5 < p_{\perp \text{ trig}} < 6.5$ GeV/c, and associated particles with $2.0 < p_{\perp \text{ assoc.}} < p_{\perp \text{ trig}}$. The two panels illustrate the existence of an elongation in $\Delta\eta$ on the same side of the azimuthal correlation (ridge), as well as the statistics, which do not allow for separation of the ridge from the jet signal. In panel a) the plot is shown in three dimensions, panel b) shows the plot from above (color on-line).

same analysis technique as before, we obtain a result shown in Figure 3. The figure presents Λ , Ξ , and Ω azimuthal correlations, with systematic uncertainties due to flow determination methods. For clarity, the uncertainty is plotted for Ξ and Ω but not for Λ . As the correlation functions are symmetric around 0 and π radians, we double our statistics by “folding” the functions around 0. Thus, the “reflected” side is shown using open symbols, while the “folded” side is shown in solid.

Figure 3 clearly shows the same-side peak for Ω baryon-triggered correlation. Moreover, within errors, there are no observable differences in peak sizes between the three species.

We study the trigger p_{\perp} and species dependence where there are sufficient statistics. Figure 4 shows unidentified charged particle, K_S^0 , Λ , Ξ , and Ω same-side yields per trigger, as a function of trigger p_{\perp} . The systematic uncertainty due to v_2 determination methods is represented by shaded bands. The yields appear to rise systematically with increasing p_{\perp} , however, there is no observable species dependence. Indeed, the Ω yield is consistent with the same-side yields of all the other particles, including unidentified charged hadrons. For the latter, we associate this behavior with jet production. Moreover, charged particle correlations are also accompanied by a similar broadening of the signal in the delta-eta space we observe for the multi-strange baryons. Thus, we conclude that if the multi-strange particles observed in most central Au+Au collisions at intermediate p_{\perp} are not made in jets, they are at least associated with jet production.

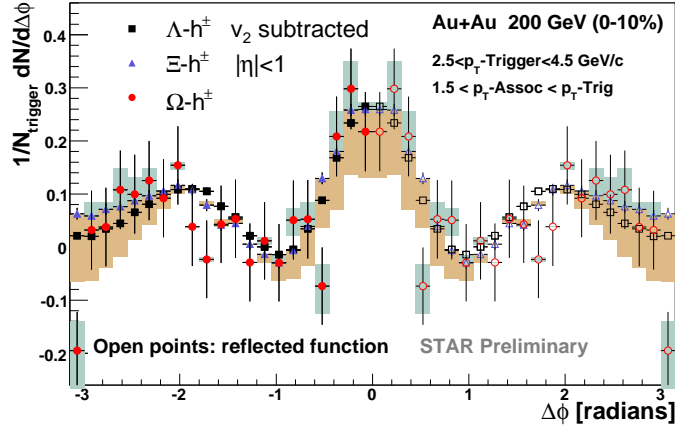


Fig. 3. $\Delta\phi$ correlation functions with Λ , Ξ , and Ω triggers at $2.5 < p_{\perp \text{ trig}} < 4.5$ GeV/c, and associated particles with $1.5 < p_{\perp \text{ assoc.}} < p_{\perp \text{ trig}}$. The blue and brown bands show the systematical error due to uncertainty in determining the v_2 coefficient.

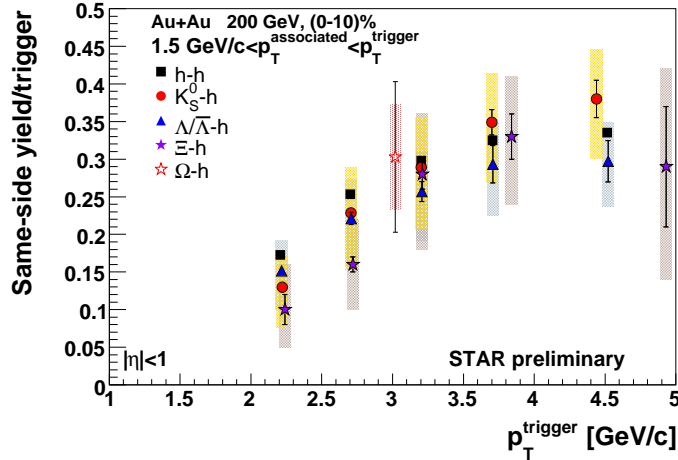


Fig. 4. Jet+Ridge yields of strange particles in 0-10% central Au+Au collisions. The shaded bands represent the systematic error due to the method used in determining the elliptic flow coefficient (color on-line). Yellow bands correspond to the error on the K_S^0 measurement, light blue – the error on the Λ measurement. The brown bands represent the error on the Ξ determination, and pink – on that of the Ω baryon.

5. Conclusions and Outlook

In this work, we have presented the first measurement of multi-strange baryon azimuthal and longitudinal correlations in relativistic heavy-ion collisions. Correlation functions were obtained in the d +Au and the central 0-10% Au+Au data sets. The yields measured for Ξ baryon correlations in the d +Au data are consistent with other strange particle results in the same data and with jet yields of singly-strange particles in the same trigger-momentum region of the most central Au+Au data. However, the triply-strange baryon correlation is the main result presented in this work. An Ω baryon correlation function was obtained in the 0-10% most central Au+Au collisions and after background subtraction, the same-side peak was compared to that of the Ξ baryon correlation and Λ baryon correlation in the same data. Contrary to predictions [3], the Ω same-side peak yield is $\sim 2\sigma$ above a null value. In fact, the per-trigger yields of the three strange baryon species, Λ , Ξ , and Ω are consistent within errors. However, there are caveats. Although there are sufficient statistics to *observe* a Ξ baryon correlation function in $\Delta\eta - \Delta\phi$ space in the most central Au+Au collisions, we are not yet ready to draw definitive conclusions as to whether there is a jet-only component of the multi-strange correlation functions. New calculations, introduced since the Ω correlation was first presented [9], predict that the same-side Ω peak is due to the jet interaction with the medium, the so-called “phantom jet” [10], not to a jet where Ω baryon is the leading particle. Further studies of multi-strange correlations in $\Delta\eta$ space will yield more details, however at present the available statistics do not allow for such measurement.

References

1. P. Koch, B. Müller, and J. Rafelski, *Phys. Rep.* **142** 167 (1986)
2. M.A.C. Lamont (for the STAR Collaboration), *J. Phys. Conf. Ser.* **50** 192 (2006)
3. R.C. Hwa and C.B. Yang, Feb. 2006 [nucl-th/0602024].
4. K.H. Ackermann et al., *Nucl. Instrum. Meth.* **A499** 624 (2003).
5. M. Anderson et al., *Nucl. Instrum. Meth.* **A499**, 659 (2003).
6. A.M. Poskanzer, S.A. Voloshin, *Phys.Rev.* **C58** 1671 (1998); N. Borghini, P.M. Dinh, and J.-Y. Ollitrault *Phys. Rev.* **C64** 054901 (2001); J. Adams et al. (STAR Collaboration), *Phys. Rev.* **C72** 114904 (2005).
7. J. Adams et al. (STAR Collaboration), *Phys. Rev. Lett.* **95**, 122301 (2005).
8. N.N. Ajitanand et al., *Phys. Rev.* **C72** 011902 (2005).
9. J. Bielcikova (for the STAR Collaboration). Talk presented at Quark Matter 2006, Shanghai, China, 14-20 Nov 2006 [nucl-ex/0701047].
10. R.C. Hwa. Talk presented at Quark Matter 2006, Shanghai, China, 14-20 Nov 2006 [nucl-th/0701018].